4DVAR AND PREDICTABILITY

Kyle Swanson
Robert Vautard
Laboratoire de Météorologie Dynamique
Paris, France

Tim Palmer
ECMWF
Reading, United Kingdom

Summary: The ability of four-dimensional variational assimilation (4DVAR) of noisy observations in a 3-layer quasi-geostrophic model to improve predictability is described. It is found that forecast lead times are extended by 5 days when observations are assimilated over a time interval extending 10 days into the past, even for weather regime transitions. For such extended assimilation time intervals, the assimilation errors are mostly concentrated on the unstable manifold (leading Lyapunov vectors) for the system. The extent to which this result holds for different observational error structures is studied. It is found that 4DVAR drastically reduces observational errors comprised of singular vector-type components that grow rapidly in the future, but that 4DVAR is ineffective at reducing observational errors comprised of Lyapunov vector-type components that have grown rapidly in the past. An exception to the general rule that 4DVAR readily reduces singular vector-type observational errors is found. If an observational error projects on the leading singular vector at the end of the assimilation time interval, and the sensitivity of that singular vector throughout the remainder of the assimilation time interval, 4DVAR does not reduce that error and rapid growth of forecast error may occur. However, the likelihood of such a scenario occurring is assessed and judged to be extremely improbable.

1. INTRODUCTION

It is well established that dynamical motions in the extra-tropical atmosphere are fundamentally chaotic. While this fact imposes an ultimate limit upon useful deterministic weather forecasts estimated at about two weeks, present performance of numerical weather prediction models shows that this limit is still far from being reached. Since weather forecasts depend strongly upon the quality of initial conditions, it is hoped that more accurate specification of those conditions will lead to substantial gains both in the quality of short range forecasts and extension of the range of useful forecasts.

One obvious route to better forecast initial conditions is improving how observational data are assimilated into numerical weather prediction models. It is widely agreed that advanced data assimilation techniques should utilize data better than current statistical interpolation techniques (Ghil and Malanotte-Rizzoli, 1991). Necessarily, this includes not only extracting as much dynamically relevant information from the data as possible, but also filtering out the spurious information, *i.e.*, the noise. Recently, one particular advanced technique – four-dimensional variational assimilation of data (4DVAR) – has been studied intensively. This interest was spawned by the work of Lewis and Derber (1986), Le Dimet and Talagrand

(1986), and Talagrand and Courtier (1987), who showed that it is feasible to perform 4DVAR with fairly realistic models. 4DVAR differs from sequential algorithms, such as variants of Kalman filtering (Kalman, 1960; Ghil and Malanotte-Rizzoli, 1991), as it seeks the best nonlinear estimate of the flow by direct explicit minimization of a scalar function measuring the misfit between the observations and the model solution over some finite time interval T_a (the assimilation time interval). The misfit, or cost function to be minimized is typically the sum of the squared observation-minus-model differences, weighted by the inverse covariance matrix of the observational errors, measured using an appropriate inner product.

While the potential of 4DVAR as an assimilation tool has attracted much attention, improvements in predictability that go along with its application have not been extensively examined. In this note, we describe to what extent 4DVAR of noisy observations in the 3-layer quasi-geostrophic (QG) model of Marshall and Molteni (1993) can improve predictability. The assimilation experiments described herein are quite straightforward. The perfect model assumption is made throughout; as such, 'observations' are generated every 6 hours arbitrarily far back in the past by adding noise to the geopotential height field of a model reference solution, and these observations are provided to 4DVAR for assimilation and forecasting. Our approach is to extend the assimilation time interval ever farther into the past, and quantify how the predictability of the system changes. However, it is well known that extending the assimilation time interval under 4DVAR for chaotic systems is fraught with danger, as secondary minima in the cost function emerge for sufficiently long assimilation time intervals T_a (Li, 1991; Gauthier, 1992; Miller et al., 1994; Pires et al., 1996). These secondary minima can 'trap' the assimilated model state away from the true best estimate of the flow. To avoid difficulties associated with the emergence of multiple minima as the assimilation time interval is extended farther into the past, the quasi-static variational assimilation (QSVA) algorithm described in Pires et al. (1996) is applied when the assimilation time interval is longer than 4 days. The results below summarize two works currently under review (Swanson et al. 1997ab).

2. PREDICTABILITY

As a first step towards understanding how much 4DVAR can improve predictability, we consider assimilation of observations in the MM93 QG model that have errors consisting of Gaussian distributed white noise with standard deviation of (60,40,20) *m* in the (200,500,800) mb QG geopotential height fields, respectively. These observations are provided uniformly over the globe every 6 hours. Since the observational error is white with respect to the squared QG geopotential height norm, or equivalently, the squared streamfunction norm, we formulate the adjoint in that norm.

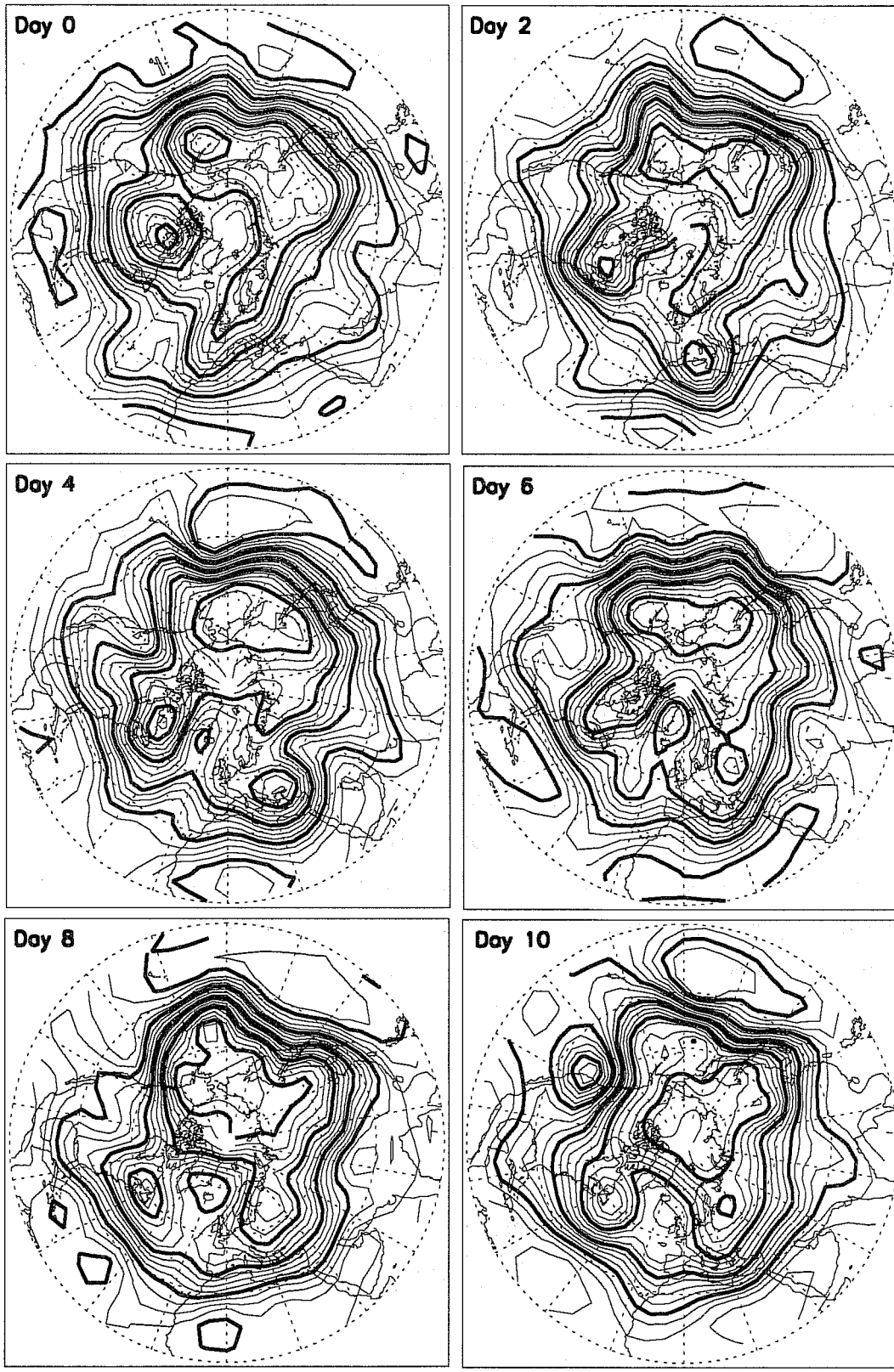

Fig. 1 Onset and maturation of the Atlantic blocking event studied herein. The contoured variable is 500 mb QG geopotential height $Z = f_0\psi/g$. Contours are every 50 m, with the 200 m contours darkened.

2.1 Weather regime transitions

For a first example, we consider whether 4DVAR can improve prediction of weather regime transitions. Weather regime transitions, such as from a zonal to a blocked flow, are well known to be difficult to predict operationally (Tibaldi and Molteni, 1990). Based upon the behavior of simple dynamical systems such as the Lorenz (1963) system, it has been argued that predictability is difficult because the flow is inherently more unstable to small perturbations during such transitions (Palmer, 1993). This instability can be quantified in any number of ways; growth of finite time singular vectors (Molteni and Palmer, 1993), local Lyapunov vectors (Trevisan and Legnani, 1995), or flow sensitivity measured by the growth of perturbations 'optimally' configured to cause regime transitions (Oortwijn and Barkmeijer, 1995) represent but three relevant measures of that instability.

The synoptic situation we consider consists of the onset and decay of a block in the European-North Atlantic sector in a QG model reference solution. Several time slices of the 500 mb height field for this reference solution are shown in Figure 1, revealing the onset and maturation of an Ω-type block in the North Atlantic between days 0 and 10. After day 10, the block decays rapidly, with the flow returning to near climatological values by day 15. Assimilation experiments for this situation are constructed as follows: to the 10 days preceding day 0 of this solution, we generate 20 different observational 'realities' by adding Gaussian white noise error to the reference solution. These observations are provided every 6 hours, and assimilation is performed over the time interval $[-T_a,0]$ for $T_a = 0$, 2, and 10 days for each realization of the observational noise. The QSVA algorithm of Pires et al. (1996) is used when $T_a = 10$ days.

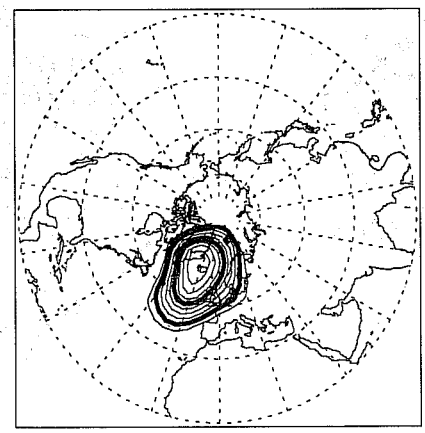

Fig. 2 Geopotential height anomaly pattern Z_B used to quantify the skill of regional prediction of weather regime transitions for the 20 manifestations of observational error. The contour interval is 25 m.

To measure the regional forecast skill, following Liu (1994) we define a blocking index by introducing the QG geopotential height anomaly pattern Z_B shown in Figure 2. This pattern was constructed by taking the low pass QG geopotential height anomaly at the peak of the block, and zeroing out that anomaly everywhere but in the European-North Atlantic sector. Given this pattern, we can then define the blocking index

$$C = \langle Z, Z_B \rangle / \langle Z_B, Z_B \rangle, \qquad (1)$$

where $Z = f_0\psi/g$ is the instantaneous 500 mb geopotential height field. We arbitrarily normalize C to vanish at day 0 and to have a value of unity at day 8 for the reference model solution. The variability of C with time for each realization of the observational error provides a quantitative measure of the skill of regional blocking prediction.

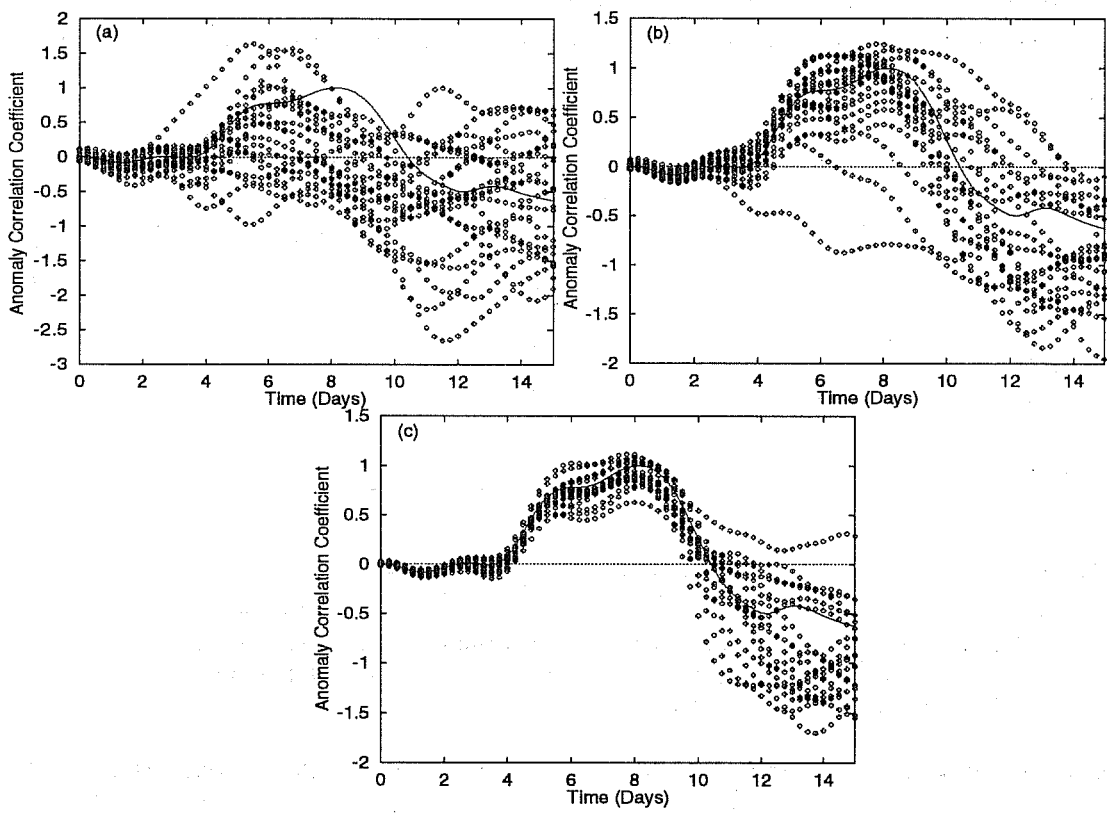

Fig. 3 Dependence of the forecast anomaly coefficient C upon T_a for the 20 realizations of observational error. (a) T_a = 0 days, (b) 2 days, and (c) 10 days. In all the figures the solid line is the anomaly correlation coefficient of the reference solution, and the impulses are the individual forecast realizations.

Examination of the forecast values of C for the 20 realizations of the observational error reveals the power of 4DVAR to improve the predictability of weather regime transitions. For T_a = 0 days (no assimilation), Figure 3(a) shows that neither the blocking onset nor its decay are well simulated. When the assimilation period is extended to T_a = 2 days, Figure 3(b) shows that the blocking onset is successfully predicted for all but two realizations of the observational error. However, the spread of the forecasts beyond day 8 indicates rather poor case-wise predictability of both the timing and speed of the decay of the block. With an

assimilation period of T_a = 10 days, however, both the onset and decay of the block are captured for all 20 realizations of the observational error. The forecast values of C only deviate significantly from the reference model solution for forecast lead times longer than 10 days.

2.2 Average predictability

Applying 4DVAR with extended assimilation time intervals also can be shown to improve the average predictive skill of the model. We next consider a 150 day model reference solution, from which noisy observations are generated every 6 hours as above. A sequential version of QSVA proposed by Pires et al. (1996) is applied to this time series to quantify the average predictability during a 100 day segment of this solution, where assimilation and forecasting are carried out every 12 hours.

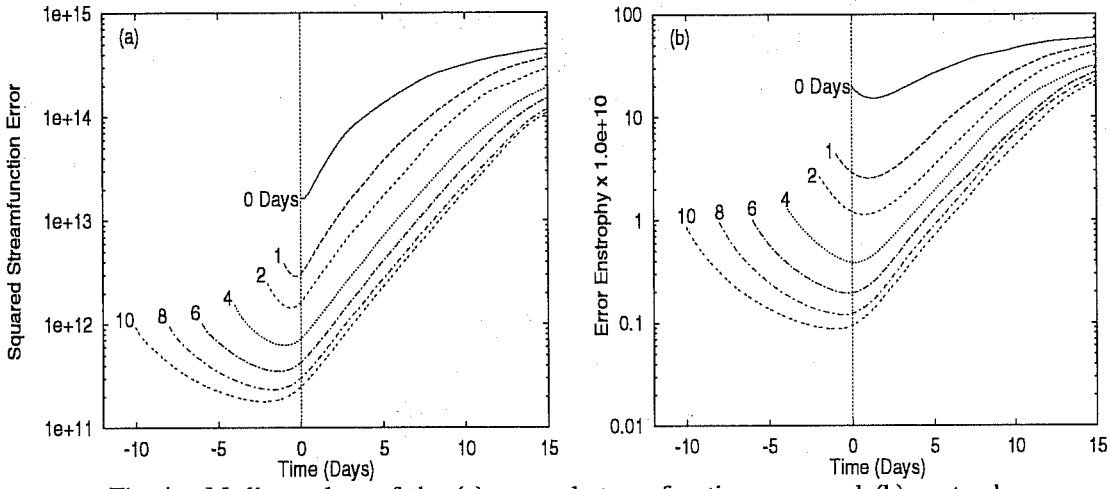

Fig. 4 Median values of the (a) squared streamfunction error and (b) enstrophy error for the 200 forecast set as a function of forecast time and of the assimilation time interval T_a.

Figure 4 shows that extending T_a from 0 to 10 days reduces the median error of the assimilated state and consequently increases the forecast skill. The error at day 0 converges to a level about 70 times smaller than the observational error in the squared streamfunction norm explicitly minimized by 4DVAR. Perhaps more surprising is the reduction in the enstrophy error by a factor of 100 over its value when no assimilation is done. This hints that error reduction by 4DVAR may not be sensitive to the choice of norm used to define the adjoint. For T_a greater than 6 days, the error growth is approximately exponential, with an error doubling time of approximately 3.5 days. Most importantly, the forecast lead times increase by 5 days as T_a is extended from 1 to 10 days. This suggests that the application of 4DVAR may allow significant advances beyond the current limits of forecast skill in operational models.

3. ASSIMILATED ERROR STRUCTURE

The improvements in predictability obtained by extending the assimilation interval are also marked by a significant change in the spectral structure of the assimilation error at the forecast initiation time. Figure 5 shows the power spectra of the squared streamfunction variance as a function of total wavenumber on the sphere at the forecast initiation time for T_a = 0, 1, 2, 4, 6, and 10 days. In addition to the substantial overall decrease in the magnitude of the error as T_a is increased, consistent with Figure 4, the shape of the spectra for long T_a indicates that the error is preferentially reduced at small scales. This is consistent with the larger reduction in error enstrophy relative to error squared streamfunction as T_a is increased. While this preferential reduction of error at small scales in no way proves that forecast error growth cascading from small to large spatial scales during the forecast is unimportant, 4DVAR does reduce error effectively even at scales not heavily weighted by the norm defining the adjoint.

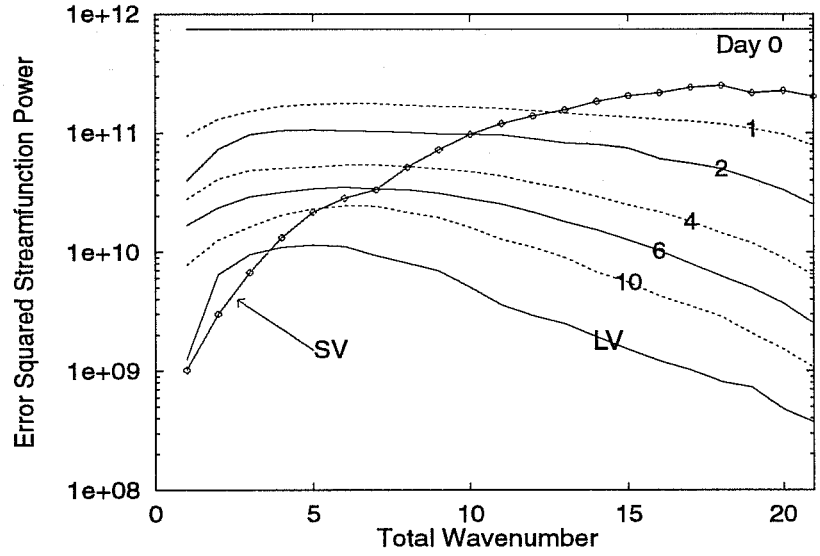

Fig. 5 Time averaged power spectra of the day 0 error in the squared streamfunction norm for the 200 forecast experiments. Individual curves are labeled by their respective values of T_a. Also included are the spectral structure of the leading Lyapunov vector (LV) and the spectral structure of the leading 2-day singular vector (SV) averaged over the 200 forecast experiments. The amplitude for these vectors is arbitrary.

Also shown in Figure 5 are the average spectra of the leading Lyapunov vector (LV), defined as the asymptotic error that has grown the fastest in the past (Legras and Vautard, 1995), and the leading 2 day future singular vector (SV), the error that will grow the fastest over the future 2 days (Molteni and Palmer, 1993). It is apparent from this Figure that the leading LV and SV have quite different spectral structures. The spectral power for the LV peaks at total wavenumber 5, with its variance tailing off for higher wavenumbers. In contrast, the spectral power for the leading SV is peaked at the smallest resolved scales of the model. Significantly, as the assimilation time interval T_a is increased, the structure of the assimilation error at the

forecast initiation time tends to resemble the leading LV. This suggests that the analysis error under 4DVAR with long assimilation time intervals projects onto the unstable manifold of the system, anticipated by the theoretical arguments of Pires et al. (1996).

To show this explicitly, we project the 200 separate analysis errors at the forecast initiation time onto the 100 leading LVs and 100 leading SVs, respectively, for varying values of T_a, and calculate the ratio between the square amplitude of the projection and that of the total error. Figure 6 shows that for short assimilation periods, the variance explained by both the leading SVs and the leading LVs is quite low. However, as T_a increases, the analysis error projection onto the LVs grows substantially, while no increase of the variance explained by the SVs is observed. Since the unstable manifold of the system is locally spanned by the LVs associated with a positive Lyapunov exponent (about 100 in the MM93 QG model), we conclude that the analysis errors for T_a = 10 days are indeed contained within the unstable manifold, while the leading SV directions do not represent this analysis error. Since the unstable manifold of a dynamical system is parallel to its attractor sheets (Eckmann and Ruelle 1983; see also Legras and Vautard 1995), we also conclude that analysis error under 4DVAR is also parallel to these sheets.

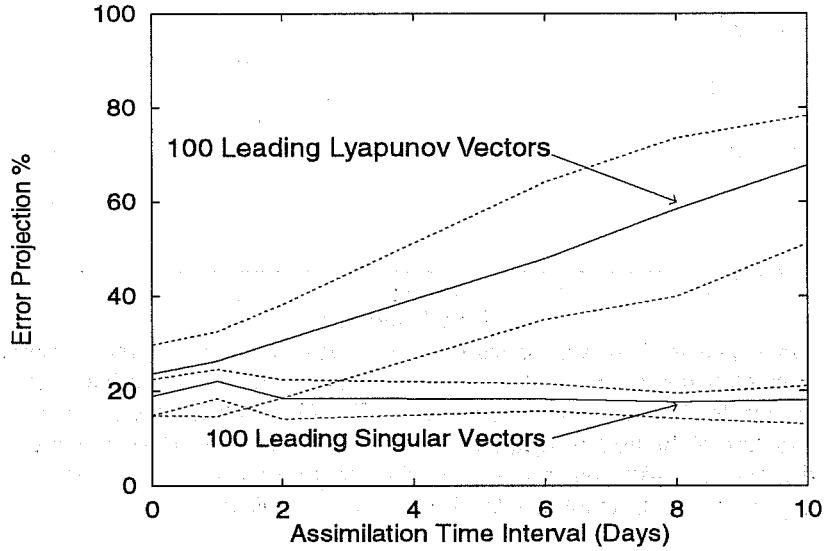

Fig. 6 Projections onto the 100 leading Lyapunov vectors and the 100 leading singular vectors as a function of assimilation time T_a. The solid lines for each are the median for the 20 experiments, and the dashed lines are the 5th and 95th percentiles.

Note, however, that this analysis error projection onto the leading LVs does not mean that non-modal singular vector-type growth is totally eliminated. This is because LVs have a nonzero (albeit small) projection onto the SVs. In order to see that this is the case, we project these 200 analysis errors at the forecast initiation time for T_a = 10 days onto the 20 leading SVs and 20 leading LVs and integrate the model forward in time from these projected errors.

Figure 7 shows the average of the squared streamfunction forecast error as a function of lead time for these projected errors. The small projection of the analysis error onto the leading 20 SVs at day 0 grows very rapidly with time, and the associated forecast error amplitude is the same as that of the forecast issued from the non-projected error after day 3. In contrast, forecasts issued from the analysis error projected onto the leading 20 LVs keep the same growth rate as the non-projected errors. The mean pattern correlation between the initially SV-projected forecast errors and the non-projected forecast errors is about 0.7. After day 3, the forecast error is evidently dominated by the component of the initial error along the leading SVs.

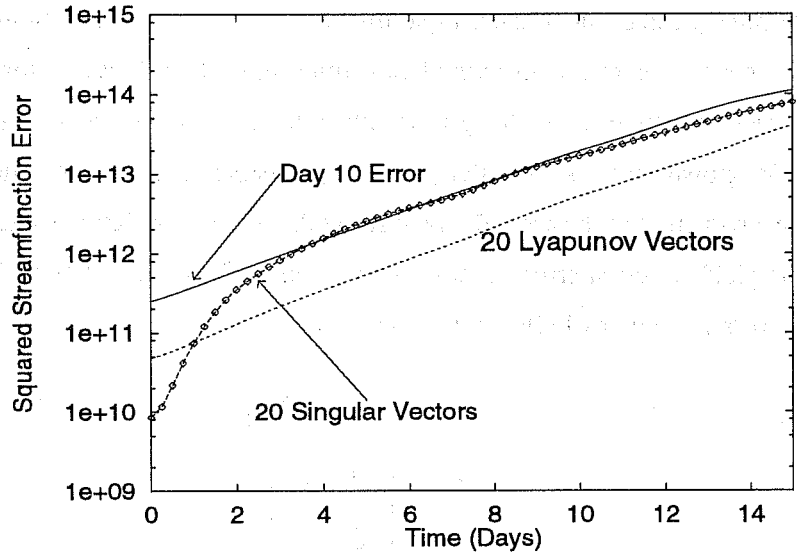

Fig. 7 Projection of 200 analysis errors for T_a = 10 days onto the 20 leading LVs and 20 leading SVs at the forecast initiation time. Also shown is the actual T_a = 10 day forecast error.

4. 4DVAR AND OBSERVATIONAL ERROR STRUCTURES

To extend our understanding of the extent to which 4DVAR can improve predictability, we next consider the performance of 4DVAR for several different observational error structures. Specifically, we consider observational errors that are comprised of either the leading SV, or the leading LV. We define an SV observational error at a time t_{obs} as the fastest growing error structure over the future two day time interval [t_{obs}, t_{obs}+2 days], while an LV observational error at a time t_{obs} is defined as the error structure that grew fastest over the past interval [t_{obs} – τ, t_{obs}] in the limit τ large.

4.1 **Distributed errors**

First, we consider the case where the observations with either SV and LV errors are uniformly distributed in time, *i.e.*, every 6 hours an observation is provided to 4DVAR for assimilation and forecasting. As above, the format of the experiments is to extend the assimilation time

interval T_a to quantify the ability of 4DVAR to reduce these two types of error. The results below are the median of 20 individual experiments, and for all cases QSVA is used when the assimilation time interval T_a is greater than 4 days to insure convergence to the absolute minimum of the cost function. Note that the observational errors for these experiments are an order of magnitude smaller than those of the previous two sections. This keeps the error time evolution linear throughout the assimilation and forecast time intervals.

Figure 8(a) shows the squared streamfunction error when the observational error at all times has the structure of the leading future 2 day SV. As expected, with no assimilation the growth of error is extremely rapid, much more rapid than the growth rate of the leading LV. Rapid growth of error also occurs for an assimilation time interval of 1 day. However, as T_a is extended to week-long time scales, the growth rate of the error decreases substantially. For T_a = 8 days, this growth rate is essentially indistinguishable from that of the leading LV. Coupled with a reduction in the assimilation error at the forecast initiation time, this reduction in growth rate yields forecast errors at day 3 that are more than a factor of 5000 smaller than the forecast errors when no assimilation is done.

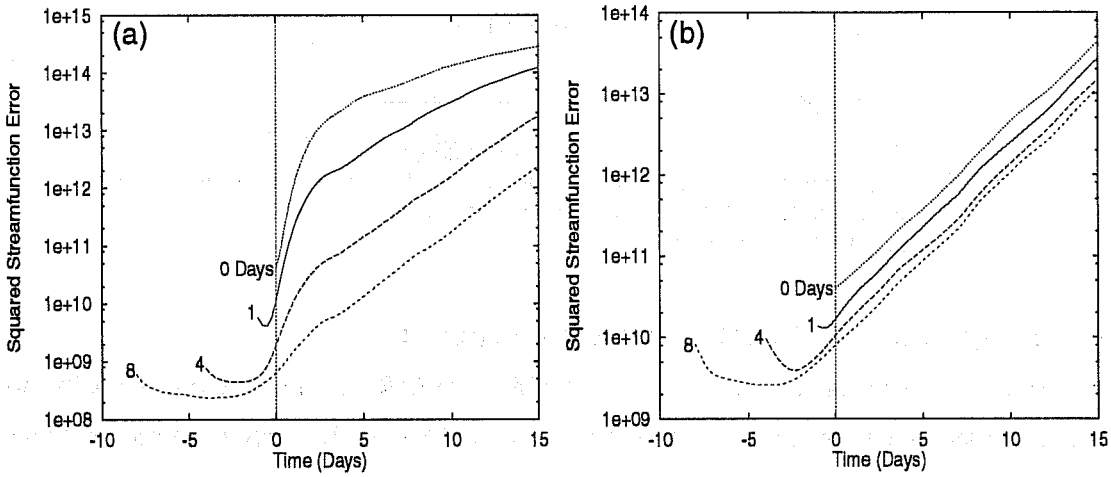

Fig. 8 Assimilation and forecast error for observations that are uniformly distributed in time but have the structure of (a) the leading SV and (b) the leading LV.

In marked contrast is the case where the observational errors lie solely in the direction of the leading LV. Figure 8(b) shows that for this case, increasing T_a leads to at most a factor of 4 reduction in the analysis error at the forecast initiation time. As noted above, since observational errors in the direction of the leading LV lie on the unstable manifold (attractor) for the system, 4DVAR is ineffective at reducing such errors. Equally, however, it should be noted that in contrast with SV error structures, LV errors do not appear to pose the danger of extremely rapid forecast error growth.

4.2 Isolated errors

While the consideration of distributed errors shows that 4DVAR readily reduces SV-type observational error structures, it is of interest to pose an even more stringent test of the ability of 4DVAR. Consider the following scenario: if day 0 is the present, we supply observations with Gaussian distributed white noise error every 6 hours for times before day -4. Then, at day -4, a 'disaster' occurs, and there is no observational data available to 4DVAR until day 0. At day 0, a single observation is made available to 4DVAR; this isolated observation has an error that lies either in the phase space direction of the leading SV or leading LV, respectively. The challenge to 4DVAR is to fill in the 4-day gap in the data and to produce an accurate forecast. To ensure significance, the results shown below are the median of 20 distinct flow states and manifestations of the observational error.

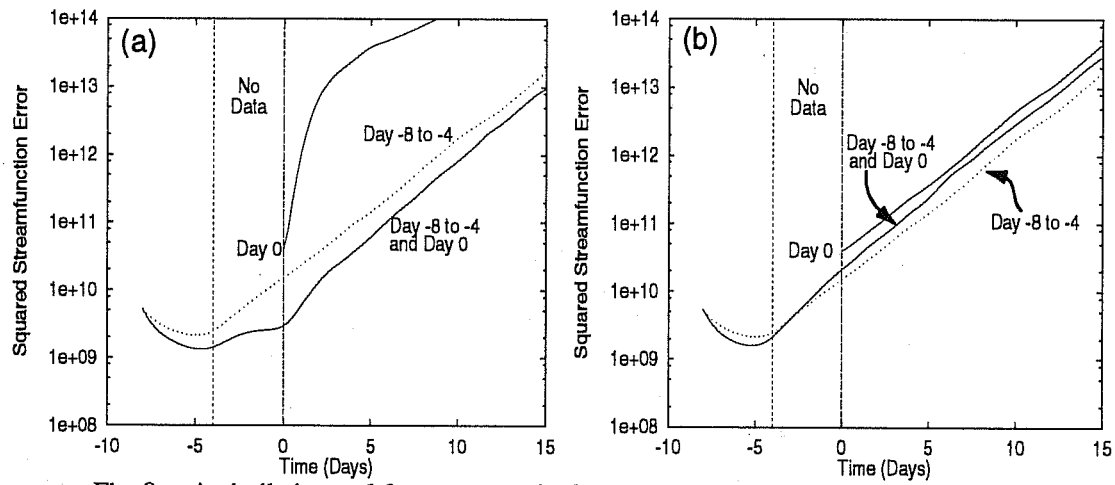

Fig. 9 Assimilation and forecast error in the squared streamfunction norm for the case where the isolated observation at day 0 has the structure of (a) the leading SV, and (b) the leading LV. Data included in the assimilation for the various curves is as indicated.

For the case where the isolated day 0 observational error lies solely in the direction of the leading SV, applying no assimilation yields a forecast error that amplifies by more than a factor of 200 over the first 2 days of the forecast. However, applying 4DVAR to the observations in the distant past (before day -4) as well as the isolated day 0 observation yields a forecast error growth rate that is essentially indistinguishable from growth rates for the leading LV in the system, and analysis errors at day 0 that are significantly smaller than when the day 0 observation is not assimilated. This shows that even when a significant amount of information about the recent past is missing, 4DVAR can extract the dynamically relevant information from an observation, effectively ignoring the rapidly growing SV component of observational error.

In contrast to the SV case, Figure 9(b) shows that when the isolated day 0 observation error has the structure of the leading LV, applying long period 4DVAR does not improve the forecast compared to the case where the day 0 observation is not assimilated. This result affirms the above results, and confirms the theoretical conjecture of Pires et al. (1996) that 4DVAR simply cannot reduce observational error projections in phase space directions that have grown rapidly in the past.

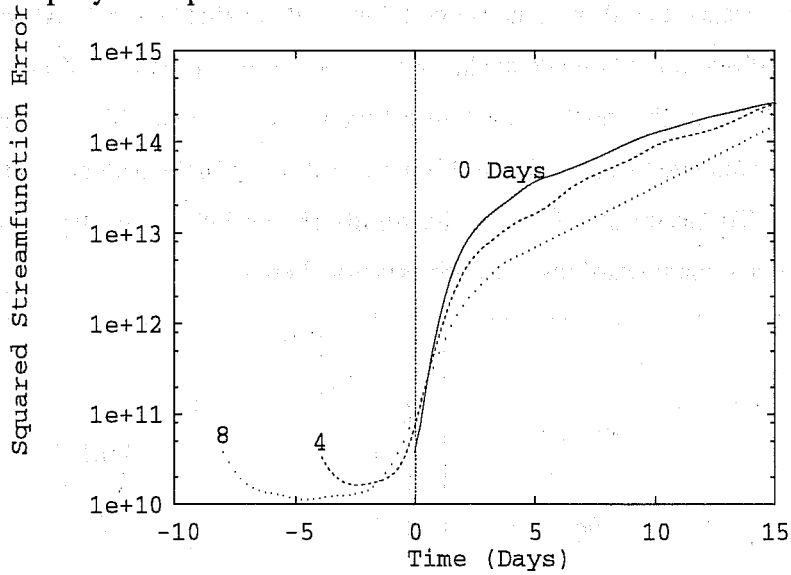

Fig. 10 Assimilation and forecast error in the squared streamfunction norm for the rapid growth scenario case. The solid line is error when no assimilation is done; the dashed line denotes $T_a = 4$ days, and the dotted line $T_a = 8$ days.

4.3 **Rapid forecast error growth scenarios**

In spite of 4DVAR's impressive ability to reduce SV-type observational errors, it should be noted that there do exist certain observational error structures that 4DVAR cannot reduce. Consider an observational error structure consisting of the leading future two day SV at day 0, and the sensitivity of that SV at every observation time in the past. As outlined by Rabier et al. (1996), the sensitivity at some time t_{obs} in the past is given by the day 0 error integrated backward in time using the adjoint model. Figure 10 shows that extending the assimilation period to 8 days reduces neither the assimilation error at day 0 nor the growth rate of the forecast error for this special type of observational error. However, it appears that 4DVAR only has difficulty with error structures that resemble this special SV/sensitivity error quite closely. Blending in a modest amount of white noise (compared to the overall probability of the noise lying in this particular phase space direction), or scrambling the phase of the sensitivity with time within the assimilation time interval both eliminate this rapidly growing forecast error. Hence, it appears that this SV/sensitivity error structure is anomalous, and that in general 4DVAR can reduce almost all rapidly growing SV-type errors.

5. CONCLUSIONS

Within the perfect model setting, 4DVAR significantly improves the quality of the assimilated state and substantially extends the lead times for useful forecasts when observations are assimilated over time scales on the order of one week. For the MM93 QG model, the improvement in the assimilated state estimate saturates at a level about 2 orders of magnitude smaller than the observational error when the assimilation time interval is extended to 10 days, and forecast lead times are extended by 5 days. This suggests that significant improvements in both assimilation quality and forecast skill may still be possible compared to their respective levels in current operational models. Long assimilation time interval 4DVAR appears to provide a viable route by which such improvements can be obtained.

Equally important to improving forecast quality is the fact that 4DVAR is particularly efficient at reducing errors in phase space directions that have not amplified in the past, *i.e.*, those directions that do not lie on the unstable manifold of the system. This is particuarly true for observational errors that project in rapidly growing singular vector phase space directions that might cause poor forecasts under current analysis schemes. Insofar as such singular vector-type errors comprise a significant portion of actual observational errors, the application of 4DVAR to produce highly accurate forecasts in operational weather prediction schemes of the future appears promising.

References

Eckmann, J.-P. and D. Ruelle, 1985: Ergodic theory of chaos and strange attractors. *Rev. Mod. Phys.*, **57**, 617-656.

Gauthier, P., 1992: Chaos and quadri-dimensional data assimilation. A study based on the Lorenz model. *Tellus*, **44A**, 2-17.

Ghil, M. and P. Malanotte-Rizzoli, 1991: Data assimilation in meteorology and oceanography. *Adv. Geophys.*, **33**, 141-266

Kalman, R., 1960: A new approach to linear filtering and prediction theory. *J. Basic. Engr.*, **82D**, 35-45.

Le Dimet, F.-X. and O. Talagrand 1986: Variational algorithms for analysis and assimilation of meteorological observations: Theoretical aspects. *Tellus*, **38A**, 97-110.

Legras, B. and R. Vautard, 1995: A guide to Liapunov vectors. *ECMWF Seminar on Predictability*, **1**, 143-156.

Lewis, J. and J.C. Derber, 1986: The use of adjoint equations to solve a variational adjustment problem with advective constraints. *Tellus*, **37A**, 309-322.

Li, Y. 1991: A note on the uniqueness problem of the variational adjustment approach to four-dimensional data assimilation. *J. Met. Soc. Japan*, **69**, 581-585.

Liu, Q., 1994: On the definition and persistence of blocking. *Tellus*, **46A**, 286-298.

Lorenz, E., 1963: Deterministic nonperiodic flow. *J. Atmos. Sci.*, **20**, 130-141.

Marshall, J. and F. Molteni, 1993: Toward a dynamical understanding of the planetary scale flow regimes. *J. Atmos. Sci.*, **50**, 1792-1818.

Miller, R.N., M. Ghil, and F. Gauthiez 1994: Advanced data assimilation in strongly nonlinear dynamical systems. *J. Atmos. Sci.*, **51**, 1037-1056.

Molteni, F. and T.N. Palmer, 1993: Predictability and finite time instability of the northern hemisphere winter circulation. *Q. J. R. Met Soc.*, **119**, 269-298.

Oortwijn, J. and J. Barkmeijer, 1995: Perturbations that optimally trigger weather regimes. *J. Atmos. Sci.*, **52**, 3932-3944.

Palmer, T.N., 1993: Extended range atmospheric prediction and the Lorenz model. *Bull. Am. Met. Soc.*, **74**, 49-65.

Pires, C., R. Vautard, and O. Talagrand 1996: On extending the limits of variational assimilation in nonlinear chaotic systems. *Tellus*, **48A**, 96-121.

Rabier, F., E. Klinker, P. Courtier, and A. Hollingsworth, 1996: Sensitivity of two-day forecast errors over the northern hemisphere to initial conditions. *Q. J. R. Met. Soc.*, **122**, 121-150.

Swanson, K. L., R. Vautard, and C. Pires 1997a: Four-dimensional variational assimilation and predictability in a quasi-geostrophic model. To appear in *Tellus*.

Swanson, K.L., T.N. Palmer, and R. Vautard 1997b: Error structure and the value of four-dimensional variational assimilation. To be submitted.

Talagrand, O. and P. Courtier , 1987: Variational assimilation of meteorological observations with the adjoint vorticity equation. I: Theory. *Q. J. R. Met. Soc.*, **113**, 1311-1328.

Tibaldi, S. and F. Molteni, 1990: On the operational predictability of blocking. *Tellus*, **42A**, 343-365.

Trevisan, A. and R. Legnani, 1995: Transient error growth and local predictability: A study in the Lorenz system. *Tellus*, **47A**, 103-117.